Nonlinear Dynamics and Systems Theory, **6**(2) (2006) 129–142

Dynamics of a Spinning Rocket with Internal Mass Flow

F.O. Eke[1*], T. Tran[2] and J. Sookgaew[3]

[1] *Department of Mechanical and Aeronautical Engineering, University of California, Davis, CA 95616, USA*
[2] *Lockheed-Martin Space Systems Co., Sunnyvale, CA 94089*
[3] *Department of Mechanical Engineering, Prince of Songkla University, Hatyai, Thailand*

Received: September 27, 2005; Revised: June 30, 2006

Abstract: One of the main simplifying assumptions made in the study of the attitude motions of a rocket-type variable mass system is that the motion of the fluid products of combustion relative to the rocket body, as these fluid particles exit the rocket's combustion chamber, remains symmetric with respect to the rocket axis, and the fluid particles have no transverse motion relative to the rocket body. This assumption brings about a tremendous simplification of the equations that govern the attitude motion of a rocket, and is thus very attractive. Yet, one recognizes that such an assumption becomes questionable if the rocket body is allowed to spin. This paper examines the validity of this common assumption. The paper attempts to reconstruct what is lost when this assumption is made, and quantifies the effects on attitude dynamics predictions. Results obtained show that this assumption is in fact reasonable. Although internal fluid whirling motion can cause deviations in spin rate predictions, the actual effects are not dramatic. There is a noticeable impact on the frequencies of the transverse angular velocity components, but the amplitude of the transverse angular velocity vector is largely unaffected.

Keywords: *Rockets; variable mass processes; attitude dynamics.*

Mathematics Subject Classification (2000): 70P05, 70M20, 34C60.

*Corresponding author: foeke@ucdavis.edu

1 Introduction

It has now become quite common to derive the equations of motion of general variable mass systems using the so-called control volume approach [1–4]. This method can capture the overall rigid-body-type motion of the system as well as the details of internal mass flow. Simplifying assumptions are introduced after the equations of motion are derived in order to bring these equations into forms that make further analyses manageable.

Rocket systems constitute one class of variable mass systems that is of interest in the aerospace field. In studying the effects of mass variation on the behavior of rocket systems, the system of interest is often assumed to comprise two phases at any given instant: a solid phase and a fluid phase. The assumptions that are traditionally made in the study of these systems include one concerning the motion of the fluid phase relative to the solid phase. Several studies [1, 3, 5] assume, explicitly or implicitly, that the motion of the fluid products of combustion relative to the solid part of the system is such that each fluid particle has constant velocity that is parallel to the rocket axis. Other studies [3, 6–8] consider that the velocity field of the fluid particles has axial symmetry, and that no "whirling motion" of the fluid phase relative to the solid phase exists. These two assumptions have to do with internal fluid flow within a rocket's combustion chamber. They stipulate that the internal motion of fluid particles relative to the rocket body is symmetric with respect to the rocket axis. In addition, the relative velocity vectors for these particles are assumed not to have a transverse component. In other words, these particles, in their motion relative to the rocket body, are assumed to be incapable of helical motion for example. This is quite reasonable for a rocket that is not spinning, but seems unreasonable for a spinning rocket. It turns out that this assumption can bring tremendous simplifications to the equations that govern rocket motion [3], and this makes the assumption quite attractive.

The goal of this work is to check the validity of this assumption; that is, to evaluate what is lost, if any, by assuming that the velocity vectors of fluid particles within a rocket's combustion chamber have no roll component relative to the rocket body. Wang and Eke [6] took a cursory look at this problem and concluded that the neglect of whirling motion does not affect transverse angular velocity magnitudes, but does affect the frequencies of these quantities. This paper builds on Wang and Eke's work, and presents the results of a more general investigation of how internal fluid whirling motion affects rocket attitude dynamics.

2 Equations of Motion

The type of system that is of interest in this study can be represented by the simple model shown in Figure 2.1. This model considers that the rocket system under study is made up of two main parts — a solid portion B, whose mass is expected to diminish with time as propellant is expended, and the fluid products of combustion F. B is taken to be rigid and symmetric about the z-axis, and is assumed to remain so as parts of it are depleted by combustion. S^* is the instantaneous mass center of the system, and always lies on the z-axis, and C is an imaginary shell that delimits the system.

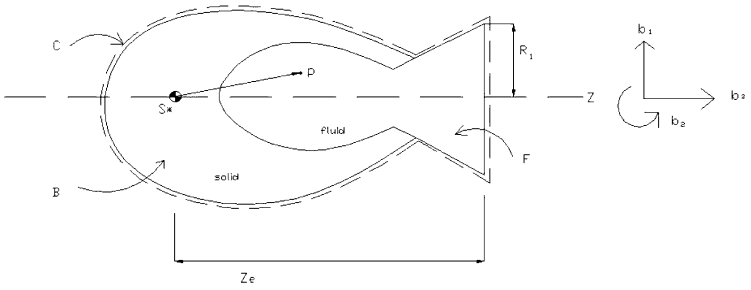

Figure 2.1. Model of a Rocket.

One version of the equation of rotational motion for this type of system has the form [3]

$$\begin{aligned}\mathbf{I}\cdot\boldsymbol{\alpha}+\boldsymbol{\omega}\times\mathbf{I}\cdot\boldsymbol{\omega}+\left(\frac{{}^{B}d\mathbf{I}}{dt}\right)\cdot\boldsymbol{\omega}+\int\limits_{C}\rho[\mathbf{p}\times(\boldsymbol{\omega}\times\mathbf{p})](\mathbf{v}\cdot\mathbf{n})\,dS\\ +\frac{{}^{B}d}{dt}\int\limits_{C}\rho(\mathbf{p}\times\mathbf{v})\,dV+\int\limits_{C}\rho(\mathbf{p}\times\mathbf{v})(\mathbf{v}\cdot\mathbf{n})\,dS+\int\limits_{C}\rho\boldsymbol{\omega}\times(\mathbf{p}\times\mathbf{v})\,dV=\mathbf{M}.\end{aligned}\tag{1}$$

In this equation, $\mathbf{I}$ represents the inertia dyadic of the system, $\boldsymbol{\omega}$ and $\boldsymbol{\alpha}$ are the inertial angular velocity and angular acceleration respectively of B, ρ is the mass density, $\mathbf{p}$ is the position vector from the system's mass center S^* to a generic particle P of the system, $\mathbf{v}$ is the velocity of P relative to the main body B, $\mathbf{n}$ is a unit outward normal to the surface C, and $\mathbf{M}$ is the resultant moment about S^* of all the external forces on the system. The left superscript on the time derivative simply indicates that the derivative is to be taken while the reference frame B is kept fixed.

If we assume that $\boldsymbol{\omega}$ has the form,

$$\boldsymbol{\omega}=\omega_1\mathbf{b}_1+\omega_2\mathbf{b}_2+\omega_3\mathbf{b}_3\tag{2}$$

and that

$$\mathbf{I}=I(\mathbf{b}_1\mathbf{b}_1+\mathbf{b}_2\mathbf{b}_2)+J\mathbf{b}_3\mathbf{b}_3\tag{3}$$

where the unit vector basis $\mathbf{b}_1$, $\mathbf{b}_2$, $\mathbf{b}_3$ is fixed in B and oriented as in Figure 2.1, then, the first three terms of equation (1) can be written as

$$\mathbf{I}\cdot\boldsymbol{\alpha}=I(\dot{\omega}_1\mathbf{b}_1+\dot{\omega}_2\mathbf{b}_2)+J\dot{\omega}_3\mathbf{b}_3,\tag{4}$$

$$\boldsymbol{\omega}\times\mathbf{I}\cdot\boldsymbol{\omega}=(J-I)\omega_3(\omega_2\mathbf{b}_1-\omega_1\mathbf{b}_2)\tag{5}$$

and

$$\left(\frac{{}^{B}d\mathbf{I}}{dt}\right)\cdot\boldsymbol{\omega}=\dot{I}(\omega_1\mathbf{b}_1+\omega_2\mathbf{b}_2)+\dot{J}\omega_3\mathbf{b}_3.\tag{6}$$

The fourth term of equation (1) has been evaluated by several authors and shown to depend on the velocity field of exhaust gas particles as they cross the nozzle exit plane. For uniform velocity profile with constant exhaust gas velocity u, the rate at which mass is lost from the system is

$$\dot{m}=-\pi\rho uR_1^2\tag{7}$$

and the fourth term can be expressed as (see for example Wang [6])

$$\int_C \rho[\mathbf{p} \times (\boldsymbol{\omega} \times \mathbf{p})](\mathbf{v} \cdot \mathbf{n})\, dS = -\dot{m}\left[\left(z_e^2 + \frac{R_1^2}{4}\right)(\omega_1 \mathbf{b}_1 + \omega_2 \mathbf{b}_2) + \frac{R_1^2}{2}\,\omega_3 \mathbf{b}_3\right] \tag{8}$$

where the distances z_e and R_1 are as shown in Figure 2.1. None of these first four terms is affected by the introduction of fluid whirling motion. This is so because the first three terms do not contain the fluid velocity vector at all, and the fourth term only involves the axial component of this velocity. We recall that whirling motion comes from the existence of a transverse component of the fluid relative velocity.

The fifth term of equation (1) vanishes if one makes the assumption that fluid flow within the system's combustion chamber has reached steady state — a generally reasonable approximation, which will be assumed to hold here. We are then left with the last two terms on the left hand side of equation (1):

$$\mathbf{M}_6 = \int_C \rho(\mathbf{p} \times \mathbf{v})(\mathbf{v} \cdot \mathbf{n})\, dS \tag{9}$$

and

$$\mathbf{M}_7 = \int_C \rho\boldsymbol{\omega} \times (\mathbf{p} \times \mathbf{v})\, dV. \tag{10}$$

Each of these contains the vector $\mathbf{v}$, which represents the velocity vector of a generic fluid particle relative to the rocket's main body. Spin motion of the rocket body introduces helical or whirling motion of the fluid particles, and this in turn influences $\mathbf{v}$, and hence both $\mathbf{M}_6$ and $\mathbf{M}_7$. We note that if whirling motion is ignored, then (see [3])

$$\mathbf{M}_6 = \mathbf{M}_7 = 0 \tag{11}$$

and equation (1) is simplified tremendously. This is one reason the "no whirling motion" assumption has remained very attractive in the study of rocket dynamics. To assess the impact of fluid whirling motion on rocket dynamics, we will start by determining expressions for the quantities $\mathbf{M}_6$ and $\mathbf{M}_7$ when whirling motion is present.

3 The Surface Integral Term

Consider a generic fluid particle within the combustion chamber of a rocket as this fluid particle crosses the nozzle exit plane. Such a particle is shown as point P in Figure 3.1. The position vector of P from the system mass center can be written as

$$\mathbf{p} = x\mathbf{e}_x + z_e\mathbf{e}_z \tag{12}$$

and its velocity relative to the rocket body B has the general form

$$\mathbf{v} = v_x\mathbf{e}_x + v_\theta\mathbf{e}_\theta + v_z\mathbf{e}_z \tag{13}$$

where $\mathbf{e}_x$, $\mathbf{e}_\theta$, and $\mathbf{e}_z$ are the unit vectors normally associated with the use of cylindrical coordinates, and are as shown in Figure 3.1. For the particle P,

$$(\mathbf{p} \times \mathbf{v})_p = -z_e v_\theta \mathbf{e}_x + (z_e v_x - x v_z)\mathbf{e}_\theta + x v_\theta \mathbf{e}_z. \tag{14}$$

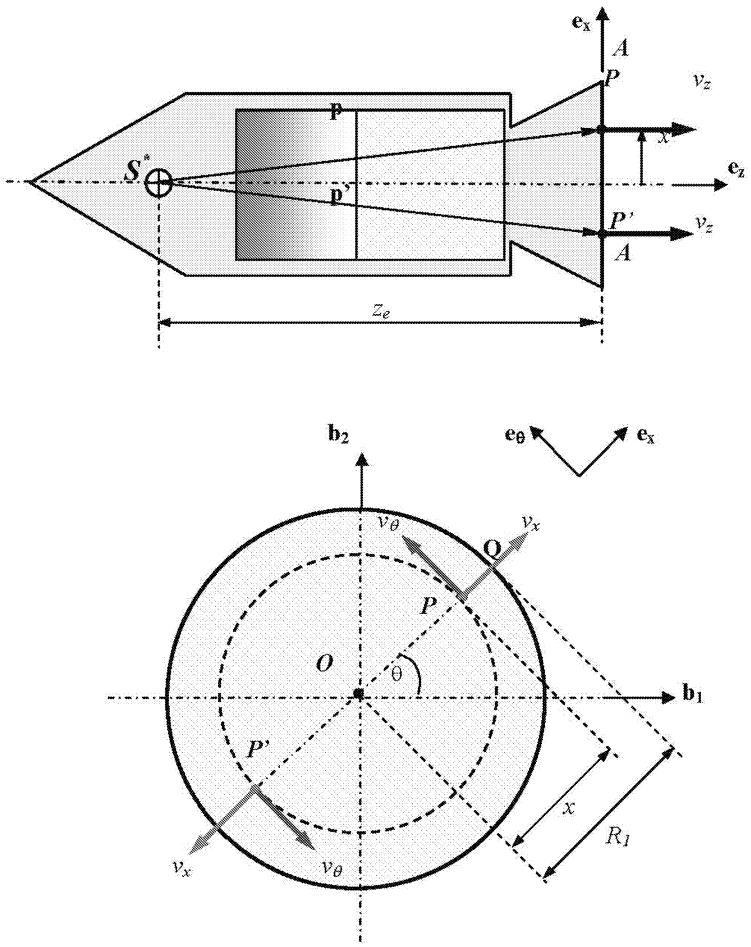

Figure 3.1. A generic fluid particle P at the nozzle exit plane.

If motion of the fluid particles relative to the rocket body is assumed to be axisymmetric with respect to the z-axis, then, for each particle such as P, there always exists another particle P' on the nozzle exit plane, located at the same radial distance x from the rocket axis, and 180 degrees away from P, and for which

$$(\mathbf{p} \times \mathbf{v})_{P'} = z_e v_\theta \mathbf{e}_x - (z_e v_x - x v_z)\mathbf{e}_\theta + x v_\theta \mathbf{e}_z. \tag{15}$$

Hence, the combined contributions of P and P' to $\mathbf{M}_6$ in equation (9) has neither a radial nor a transverse component, so that one need only evaluate the axial component of the surface integral $\mathbf{M}_6$. In other words,

$$\mathbf{M}_6 = (\mathbf{M}_6 \cdot \mathbf{e}_z)\mathbf{e}_z = \mathbf{e}_z \int_C \rho \mathbf{p} \cdot (\mathbf{v} \times \mathbf{e}_z)(v_z)\, dS = \mathbf{e}_z \int_C \rho x v_\theta v_z \, dS. \tag{16}$$

The axisymmetry assumption stated above also leads to the conclusion that neither v_z nor v_θ depends on the angle θ. However, both can depend on the distance x from the rocket axis. We can re-write equation (16) as

$$\mathbf{M}_6 = \left[2\pi\rho \int_0^{R_1} x^2 v_\theta u \, dx\right] \mathbf{b}_3. \tag{17}$$

This expression assumes a constant axial velocity u for fluid particles as well as a constant fluid density over the nozzle exit plane.

To make further progress with equation (17), the manner in which v_θ varies with x must be determined. To this end, we will assume that at steady state, the motion of a typical fluid particle relative to the rocket body, as the particle moves towards the nozzle exit plane, is such that the path of the particle has the approximate shape of a helix centered on the rocket axis. We immediately recognize that the transverse component of the velocity of such a particle is influenced mainly by the spin motion of the rocket body. This leads us to start the process of determining an expression for v_θ by making the additional simplifying assumption that the axial motion of the fluid particles is decoupled from their transverse motion. This means that the transverse motion of the fluid particles can be understood by considering only the spin motion of the rocket body. Thus, we consider in Figure 3.2, that initially, the rocket body B, including the nozzle and the fluid it contains, is stationary. Next, B is given a spin rate ω_3 as shown. Friction causes the fluid particle Q in contact with the nozzle wall to acquire an inertial velocity $\omega_3 R_1$ in the transverse direction, while the fluid particle O on the spin axis remains stationary. Those fluid particles between O and Q acquire speeds that vary between zero and $\omega_3 R_1$. For the range of spin rates normally encountered in rocket dynamics, the speed distribution between O and Q would be linear, and the relationship between the speed of the fluid particle P at a distance x from O and the fluid particle at Q would be

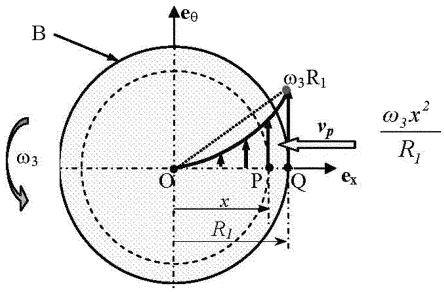

Figure 3.2. Fluid velocity distribution.

$$v^P / v^Q = x / R_1 \tag{18}$$

so that

$$\mathbf{v}^P = (x/R_1) v^Q \mathbf{e}_\theta = \omega_3 x \mathbf{e}_\theta. \tag{19}$$

On the other hand, the fictitious particle P_O of B that is coincident with the fluid particle P at the instant under consideration also has velocity

$$\mathbf{v}^{P_O} = \omega_3 x \mathbf{e}_\theta. \tag{20}$$

P would then have zero velocity relative to the rocket body; a fact that seems at odds with what would be expected if such an experiment were actually performed.

The decoupling of the axial fluid velocities from the transverse velocities has one major flaw — it implies that one is dealing with linear phenomena. Furthermore, the assumption that the velocity distribution between points O and Q is linear requires that the flow be laminar (not turbulent). What is most likely in reality is that the combination of very high axial fluid velocities found inside rocket combustion chambers, together with the relatively slow transverse motion of the fluid particles, as well as the changing combustion chamber geometry will result in overall turbulent and complex flow of the fluid products of combustion. It is thus most unlikely that spinning of the rocket body will introduce a linear distribution of transverse fluid velocities between points O and Q; in other words, the relative transverse speeds for the fluid particles are not likely to be zero. The velocity function v_θ is likely to be quite complex, with no simple closed form expression.

One way to move this analysis forward is to make reasonable guesses for the function v_θ. We adopt this approach and assume that the velocity distribution between points O and Q of Figure 3.2 is not linear, but parabolic. One then finds that

$$\mathbf{v}^P = (\omega_3 x^2/R_1)\mathbf{e}_\theta \tag{21}$$

and hence, the transverse speed of the general fluid particle P relative to the spinning body B becomes

$$v_\theta = \omega_3 x\left(\frac{x}{R_1} - 1\right). \tag{22}$$

We now substitute equation (22) into (17) to obtain

$$\mathbf{M}_6 = \left[2\pi \int_0^{R_1} \rho\left(\frac{x}{R_1} - 1\right)\omega_3 u x^3 dx\right]\mathbf{b}_3 = -\frac{\pi\rho u\omega_3 R_1^4}{10}\,\mathbf{b}_3 = \frac{\dot{m}\omega_3 R_1^2}{10}\,\mathbf{b}_3. \tag{23}$$

Clearly, $\mathbf{M}_6$ will have some influence on the spin rate but will not affect the transverse components of the rocket's angular velocity.

4 The Volume Integral Term

In this section, we determine an explicit expression for the seventh term of equation (1). This term is also shown as equation (10) above, and is a volume integral to be taken over the entire region of the combustion chamber, where fluid flow occurs. We note that this region's volume varies with time as propellant burn progresses, a fact that complicates the evaluation of the integral.

For a general axisymmetric combustion chamber such as the one shown in Figure 4.1, the vector $\mathbf{M}_7$ can be written as

$$\mathbf{M}_7 = \boldsymbol{\omega} \times \int_C (\rho\mathbf{p} \times \mathbf{v})\, dV = \boldsymbol{\omega} \times \boldsymbol{\Gamma} \tag{24}$$

where

$$\boldsymbol{\Gamma} = \int_C (\rho\mathbf{p} \times \mathbf{v})\, dV. \tag{25}$$

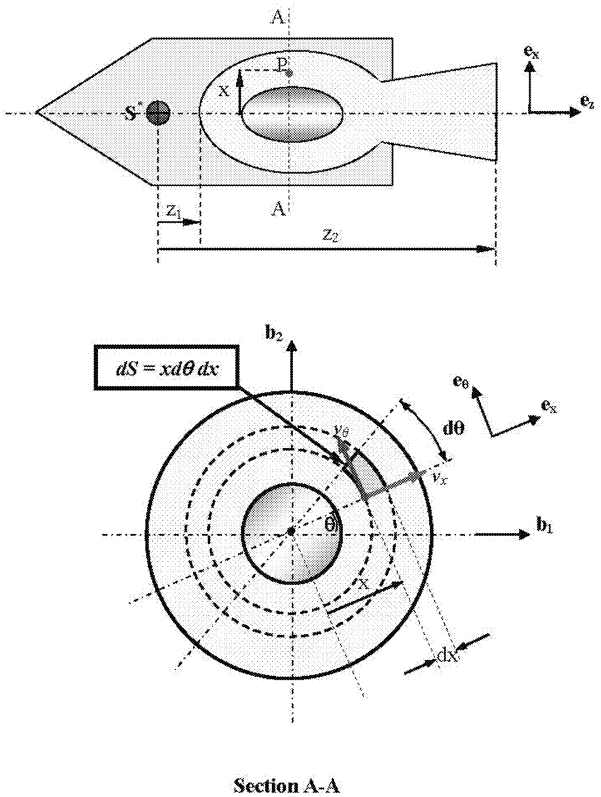

Figure 4.1. General axisymmetric combustion chamber.

We can let $\mathbf{p}$, which represents the position vector from the system mass center to a generic fluid particle P inside the combustion chamber, be

$$\mathbf{p} = x\mathbf{e}_x + z\mathbf{e}_z \tag{26}$$

while a general expression for the velocity of P remains as given in equation (13). The axisymmetric nature of both the combustion chamber and the fluid flow therein allows us to invoke the same arguments presented in the evaluation of $\mathbf{M}_6$, and these lead us to conclude that $\mathbf{\Gamma}$ is parallel to $\mathbf{e}_z$ or $\mathbf{b}_3$. Hence, equation (25) becomes

$$\mathbf{\Gamma} = \mathbf{e}_z \int_C (\rho\mathbf{p} \times \mathbf{v}) \cdot \mathbf{e}_z \, dV = \mathbf{b}_3 \int_C \rho x^2 v_\theta \, dx \, d\theta \, dz. \tag{27}$$

Equations (2) and (27) are now substituted into (24), and, assuming that the fluid density is constant at steady state, we obtain (see also Figure 4.1)

$$\mathbf{M}_7 = \left(2\pi\rho \int_{z_1}^{z_2} \int_x x^2 v_\theta \, dx \, dz \right) (\omega_2 \mathbf{b}_1 - \omega_1 \mathbf{b}_2). \tag{28}$$

Because $\mathbf{M}_7$ has no $\mathbf{b}_3$ component, it cannot have any influence on the spin rate.

The integral in equation (28) depends on the shape of the combustion chamber, and this in turn depends on the propellant burn type. We will thus need to stipulate a specific propellant burn scenario before the corresponding expression for $\mathbf{M}_7$ can be determined. The idealized propellant burn geometries that are closest to what obtains in real systems are those that have been described in the literature [7–9] as the end burn, the radial burn, and the uniform burn. Even for these idealized burn patterns, the true shape of the combustion chamber during the propellant burn remains quite complex. To simplify the task of evaluating the volume integral $\mathbf{M}_7$, we restrict this part of the analysis to a rocket model often referred to as the variable mass cylinder [7]. This is a very simple model that considers a rocket to be a solid right circular cylinder, made entirely of combustible material, and that burns while it flies around in space.

The end burn is the most useful propellant burn geometry for the variable mass cylinder. To see why this is so, we direct attention to Figure 4.2, which shows a typical rocket system that consists of the payload and several stages of the propulsion system. The rocket motor for each stage carries solid or liquid propellant that burns to generate propulsive force. Typically, solid fuel is burnt from inside out, somewhat similar to what we have referred to as radial burn. However, the fact that the fuel is generally located close to one end of the rocket system, means that the effect of this burn on the overall system geometry and mass/inertia properties, is reasonably well approximated by the end burn when the overall system is modeled as a cylinder. We will therefore only consider the end-burn whenever we model a rocket as a burning cylinder.

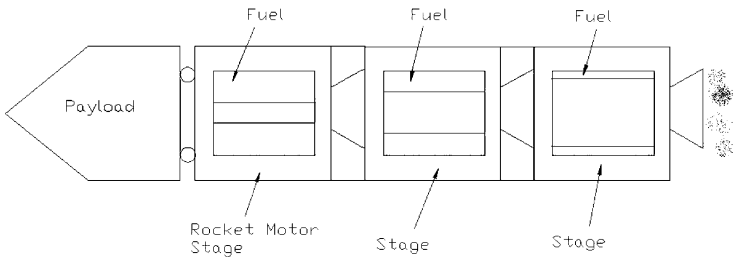

Figure 4.2. Typical rocket system.

For the end burning cylinder, the combustion chamber at any given instant has the shape of a cylinder of radius R, and whose length varies uniformly with the burn, as shown in Figure 4.3. In this case, $\mathbf{M}_7$ becomes

$$\begin{aligned}\mathbf{M}_7 &= \left(2\pi\rho \int_z^L \int_0^R x^2 v_\theta \, dx \, dz\right)(\omega_2 \mathbf{b}_1 - \omega_1 \mathbf{b}_2) \\ &= 2\pi\rho(L-z)\left(\int_0^R x^2 v_\theta \, dx\right)(\omega_2 \mathbf{b}_1 - \omega_1 \mathbf{b}_2).\end{aligned} \tag{29}$$

We assume that the expression obtained for v_θ in the previous section [see equation (22)] holds here, so that

$$\mathbf{M}_7 = -\frac{1}{10}\,\pi\rho R^4 (L-x)\omega_3(\omega_2 \mathbf{b}_1 - \omega_1 \mathbf{b}_2). \tag{30}$$

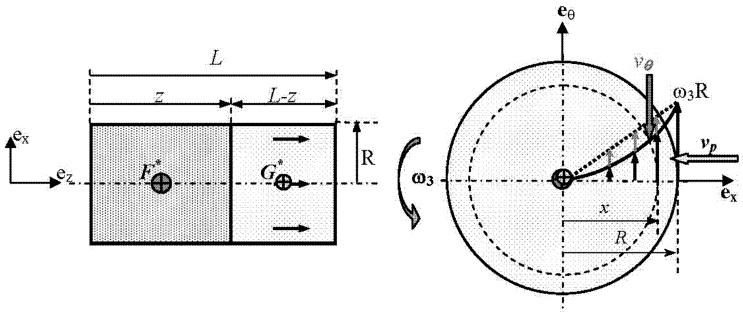

Figure 4.3. The end burning cylinder.

The mass flow rate can be introduced into equation (30), as was done earlier for the vector $\mathbf{M}_6$. For uniform exit velocity profile, $\mathbf{M}_7$ then becomes

$$\mathbf{M}_7 = \frac{\dot{m}R^2(L-z)}{10u}\,\omega_3(\omega_2\mathbf{b}_1 - \omega_1\mathbf{b}_2). \tag{31}$$

5 Scalar Equations of Attitude Motion

Now that the explicit expression for each term of equation (1) has been determined, including those contributed by fluid whirling motion, we are in a position to write the complete scalar equations of rotational motion. Using equations (4), (5), (6), (8), (23), and (31), and assuming the external moment $\mathbf{M}$ is zero, equation (1) can be broken into its scalar components along the $\mathbf{b}_1$, $\mathbf{b}_2$, and $\mathbf{b}_3$ directions respectively as follows:

$$I\dot{\omega}_1 + \left[\dot{I} - \dot{m}\left(z_e^2 + \frac{R^2}{4}\right)\right]\omega_1 + [(J-I)\omega_3 + \Delta\omega_3]\omega_2 = 0, \tag{32}$$

$$I\dot{\omega}_2 + \left[\dot{I} - \dot{m}\left(z_e^2 + \frac{R^2}{4}\right)\right]\omega_2 - [(J-I)\omega_3 + \Delta\omega_3]\omega_1 = 0, \tag{33}$$

and

$$J\dot{\omega}_3 + \left(\dot{J} - \dot{m}\,\frac{R_1^2}{2}\right)\omega_3 + \frac{1}{10}\,\dot{m}R_1^2\omega_3 = 0 \tag{34}$$

where

$$\Delta = \frac{\dot{m}(L-z)R^2}{10u}. \tag{35}$$

Equations (32) and (33) are only valid for the cylinder model, while equation (34) holds for a more general representation of a rocket because the term $\mathbf{M}_7$ that forced a return to the cylinder model contributes nothing to (34). The Δ term in equations (32) and (33), and the last term on the left hand side of (34) are contributed by fluid whirling motion.

6 Spin Motion

We now assess how the rocket's spin rate is affected by the inclusion of the extra term due to fluid whirling motion. The spin rate is obtainable from equation (34) and has the form

$$\frac{\omega_3(t)}{\omega_3(0)} = \exp\left[-\int_0^t \frac{\psi(t)}{J}\, dt \right] \tag{36}$$

where

$$\psi(t) = \psi_1(t) + \psi_2(t) + \psi_3(t) = \dot{J} - \frac{1}{2}\,\dot{m}R_1^2 + \frac{1}{10}\,\dot{m}R_1^2 \tag{37}$$

with

$$\psi_1(t) = \dot{J}, \quad \psi_2(t) = -\frac{1}{2}\,\dot{m}R_1^2, \quad \psi_3(t) = \frac{1}{10}\,\dot{m}R_1^2. \tag{38}$$

We know from equation (36) that the spin rate increases or decreases depending on the sign of $\psi(\tau)$: a positive sign indicates a decrease in spin rate, while a negative sign points to an increase in spin rate. The rate of change of the system's axial moment of inertia $\dot{J}$ and the mass flow rate $\dot{m}$ are negative quantities. Hence, $\psi_1(\tau)$ will tend to augment the spin rate, while $\psi_2(\tau)$ does the opposite. $\psi_3(\tau)$, which is contributed by internal fluid whirling motion, is a negative quantity. This means that fluid whirling motion tends to increase the spin rate value. In other words, an analysis that ignores fluid whirling motion will predict spin rate values that are less than those resulting from an analysis in which whirling motion is accounted for. In the remainder of this section, $\omega_3(t)$ will continue to represent the spin rate solution when fluid whirling motion is accounted for, while $\omega_{3nw}(t)$ will be used for the spin rate solution when whirling motion is neglected (i.e. when $\psi_3(\tau)$ is dropped).

For the specific case of a variable mass cylinder in end burn (see Figure 4.3),

$$\begin{aligned} \frac{\omega_3(t)}{\omega_3(0)} &= \exp\left[-\int_0^t \frac{\dot{J}}{J}\, dt + \frac{R^2}{2}\int_0^t \frac{\dot{m}}{J}\, dt - \frac{R^2}{10}\int_0^t \frac{\dot{m}}{J}\, dt \right] \\ &= \exp\left[-\ln\frac{J(t)}{J(0)} + \ln\frac{m(t)}{m(0)} - \frac{1}{5}\ln\frac{m(t)}{m(0)} \right] = \exp\left(-\frac{1}{5}\ln\frac{m(t)}{m(0)} \right). \end{aligned} \tag{39}$$

Observe that

$$\omega_{3nw}(t) = \omega_3(0). \tag{40}$$

Hence, if whirling motion is not accounted for, the spin rate for a spinning rocket is predicted to remain constant at its initial value. This is in fact quite close to what is observed in real flight. On the other hand, if whirling motion is accounted for, the predicted spin rate is somewhat higher. The percentage deviation of $\omega_3(t)$ from $\omega_{3nw}(t)$ is

$$D = \frac{\omega_3 - \omega_{3nw}}{\omega_{3nw}}\, 100 = 100\left[\left(\frac{m(0)}{m(t)} \right)^{1/5} - 1 \right] = 100\left[\left(\frac{L}{z} \right)^{1/5} - 1 \right]. \tag{41}$$

An equivalent z/L for a real rocket is very small, hence D is very small. We conclude then that accounting for whirling motion does not change the predicted spin rate by much.

7 Transverse Motion

We continue the investigation of the effects of internal whirling motion of fluid products of combustion on the attitude behavior of variable mass systems of the rocket type by examining the lateral or transverse attitude motion of such systems. The interest here is in the evolution with time, of the transverse angular velocity components ω_1 and ω_2 as the rocket's propellant burns. The variables ω_1 and ω_2 are governed by equations (32) and (33), which we combine and re-write in the form

$$\dot{\omega}_c = -\frac{1}{I}\left\{\left[\dot{I} - \dot{m}\left(z_e^2 + \frac{R^2}{4}\right)\right] - j[(J-I)+\Delta]\,\omega_3\right\}\omega_c \tag{42}$$

where

$$\omega_c = \omega_1 + j\omega_2 \tag{43}$$

with

$$j = \sqrt{-1} \tag{44}$$

and ω_3 is now a known function of time.

Equation (42) is integrated, leading to

$$\omega_c(t) = \omega_c(0)\Lambda(t)\exp[j\Theta(t)] \tag{45}$$

where

$$\Theta(t) = \int_0^t \frac{(J-I)+\Delta}{I}\,\omega_3\,dt \tag{46}$$

and

$$\Lambda(t) = \exp\left[-\int_0^t \frac{\dot{I} - \dot{m}(z_e^2 + R^2/4)}{I}\,dt\right]. \tag{47}$$

Equation (45) indicates that both components of the transverse angular velocity vector oscillate with varying amplitude and varying frequency. The function $\Lambda(t)$ controls the amplitude of these oscillations while Θ determines the frequency. We recall that in the differential equations governing ω_1 and ω_2 (see equations (32) and (33)), the terms containing Δ are the only terms contributed by fluid whirling motion. $\Lambda(t)$ contains no such terms, but Θ does. Hence, we can state that internal fluid whirling motion has no effect on the amplitude of the transverse angular velocity vector. However, the frequency predicted for the transverse angular velocity components when the no-whirling-motion assumption is made will generally differ from that obtained when whirling motion is accounted for.

From equation (46), we can write

$$\Theta(t) = \Theta_1(t) + \Theta_2(t) \tag{48}$$

where

$$\Theta_1(t) = \int_0^t \frac{J-I}{I}\,\omega_3\,dt \tag{49}$$

and

$$\Theta_2(t) = \int_0^t \frac{\Delta}{I}\,\omega_3\,dt = \int_0^t \frac{\dot{m}(L-z)R^2}{10uI}\,\omega_3\,dt. \tag{50}$$

If fluid whirling motion is ignored, $\Theta_2(t) = 0$. Otherwise, it is a negative quantity that increases in absolute value with time. On the other hand, the sign of $\Theta_1(t)$ depends on whether the overall rocket system is oblate or prolate in shape. For an oblate system, $J/I > 1$, and $\Theta_1(t)$ is positive and increases with time. For a prolate system — the most likely case — $J/I < 1$, and $\Theta_1(t)$ is negative and increases in absolute value with time. In summary, if fluid whirling motion is ignored, only $\Theta_1(t)$ determines the frequency. This means that the frequency of the transverse angular velocity will increase with time both for prolate and oblate systems. On the other hand, if whirling motion is accounted for in the modeling of the system under study, then the frequency will increase with time for prolate systems, and will be higher at all times than that predicted for no-whirling-motion. This is due to the fact that $\Theta_2(t)$ is then non-zero, and also the fact that the quantity $\omega_3(t)$ appearing in equation (50) is always greater for whirling motion than for no-whirling motion.

For oblate systems, $\Theta_1(t)$ will be positive and growing, while $\Theta_2(t)$ is negative and decreasing (growing in absolute value). So, the frequency could grow or decrease with time. What is clear though, is that the frequency in this case will always be less than the frequency for prolate systems. Finally, we observe that the frequency predicted when whirling motion is accounted for could, in this case, be less than that predicted when whirling motion is neglected.

8 Conclusion

This study evaluates the impact that helical motion of fluid products of combustion within the combustion chamber of a rocket can have on the attitude dynamics of rocket systems. Analysis performed using a variable mass cylinder as a model for rocket systems shows that spin rate predictions made with the no-whirling-motion assumption will be less than those which would have been predicted if whirling motion were properly accounted for. However, the deviation from the "correct" spin rate will be quite small.

The amplitude of a rocket's transverse angular velocity is unaffected by fluid whirling motion. The only impact that fluid whirling motion has on a rocket's transverse rotational motion shows up in the frequencies of the transverse angular velocity components of the rocket body. The degree to which these frequencies are affected also depends on the ratio of the system's spin inertia to its transverse inertia; in other words, on whether the system is prolate or oblate. If whirling motion is accounted for in the modeling of a prolate rocket system, the frequency of the transverse angular velocity components will be found to increase with time, and will be higher at all times than the frequency predicted with a no-whirling-motion assumption. For oblate systems, a model that takes whirling motion into account will show that the frequency of rocket transverse motion can increase or decrease with time, but will always be less than the frequency for a prolate system. Ignoring whirling motion can result in a higher or lower frequency.

References

[1] Meirovitch, L. General motion of a variable mass flexible rocket with internal flow. *Journal of Spacecraft and Rockets* **7**(2) (1970) 186–195.
[2] Belknap, S.B. A general transport rule for variable mass dynamics. *AIAA Journal* **10**(9) (1972) 1137–1138.
[3] Eke, F.O. and Wang, S.M. Equations of motion of two-phase variable mass systems with solid base. *Journal of Applied Mechanics* **61**(4) (1994) 855–860.
[4] Eke, F.O. and Mao, T.C. On the dynamics of variable mass systems. *The Int. J. of Mechanical Engineering Education* **30**(2) (2002) 123–137.
[5] Thomson, W.T. Equations of motion for the variable mass system. *AIAA Journal* **4**(4) (1966) 766–768.
[6] Wang, S.M., and Eke, F.O. Rotational dynamics of axisymmetric variable mass systems. *J. of Appl. Mechanics* **62**(4) (1995) 970–974.
[7] Mao, T.C. and Eke, F.O. Attitude dynamics of a torque-free variable mass cylindrical body. *The Journal of the Astronautical Sciences* **48**(4) (2000) 435–448.
[8] Sookgaew, J. and Eke, F.O. Effects of substantial mass loss on the attitude motions of a rocket-type variable mass system. *Nonlinear Dynamics and Systems Theory* **4**(1) (2004) 73–88.
[9] Eke, F.O. and Sookgaew, J. Influence of propellant burn pattern on the attitude dynamics of a spinning rocket. *Nonlinear Dynamics and Systems Theory* **5**(3) (2005) 251–264.